Molecular Thermodynamics of Solubilities in Gas Antisolvent Crystallization

David J. Dixon and Keith P. Johnston
Dept. of Chemical Engineering, University of Texas at Austin, Austin, TX 78712

An expanded liquid molecular thermodynamic model is developed to predict the solubilities of pure solids in a liquid expanded with a gaseous antisolvent. Experimental data are presented for systems containing naphthalene, phenanthrene, and a mixture of both in toluene expanded with a gas antisolvent, CO_2. The pressure range is 1 to 64 bar and the temperature is 25°C. The data are predicted accurately with regular solution theory up to moderate pressures, but not at the higher pressures where the liquid phase is nearly pure CO_2. In contrast, the new expanded liquid equation of state model describes the wide range of behavior from the nearly ideal liquid solution at ambient pressure to the highly nonideal compressible fluid at elevated pressures. As a result, it predicts solubilities accurately over three orders of magnitude by using only binary interaction parameters. The implications of the phase behavior on fractional crystallization with a gas antisolvent are discussed.

Introduction

Gaseous CO_2 is quite soluble in a number of organic solvents at pressures from 10 to 100 bar. The dissolved gas expands the liquid phase, decreasing its cohesive energy density (solvent strength) substantially. The gas may be used as an antisolvent to crystallize solutes from the liquid phase as a function of pressure. A method has been developed (Zsigismondy and Bachmann, 1918; Strathmann and Kock, 1977) of introducing a vapor-phase precipitant to form symmetric structured polymer membranes, by precipitation from a polymer casting solution. Stahl et al. (1988) cites additional references from the late 1930's through the 1950's where this procedure was proposed for separations. Irani et al. (1982), McHugh and Guckes (1985), and others showed that the lower critical solution temperature (LCST) of a polymer solution could be significantly lowered by the addition of a supercritical fluid antisolvent. Yu et al. (1989) examined phase behavior of supercritical carbon dioxide and bitumen and found that dissolved CO_2 can cause precipitation of solids. The addition of high-pressure gases and supercritical fluids to multicomponent mixtures of solids can depress melting points and eutectics (White and Lira, 1989). Another important advancement is the work of Gallagher et al. (1989) that demonstrated that the rate of addition of a gas antisolvent and/or pressure may be programmed to control crystal morphology, particle size, and particle size distribution over a wide range. Chang and Randolph (1990) observed that the solubilities of β-carotene and acetaminophen in liquid solvents, which were expanded with CO_2, could be varied significantly with pressure.

It is informative to compare gas antisolvent recrystallization with a complementary technique, so-called rapid expansion from supercritical fluid solution (RESS), which has been described in a recent review article (Tom and Debenedetti, 1991). A supercritical fluid solution may be expanded rapidly (<10 ms) to produce an unusually high supersaturation ratio, for example, 10^5. As a result, nucleation is uniform, and narrow particle size distributions have been observed even for submicron particles. Compared with conventional solution crystallization, RESS offers several advantages. The product can be highly monodisperse, it is not contaminated with solvent, and waste solvent streams are reduced. While RESS has been used for diverse materials including ceramic precursors, pharmaceuticals, polymers, and a few inorganic and organic compounds, there is a stringent requirement that the solute be soluble in the supercritical fluid. Most polar and many nonpolar compounds are only sparingly soluble or are insoluble in CO_2, and often it will be necessary to use a fluid with a high critical temperature or to use a cosolvent such as alcohol or a surfactant (Dobbs and Johnston, 1987). Higher temperatures, however, could be detrimental to the product, and in some cases cosolvents can have undesirable effects on the nucleation.

At ambient temperature, gas antisolvent crystallization with

Correspondence concerning this article should be addressed to K. P. Johnston.

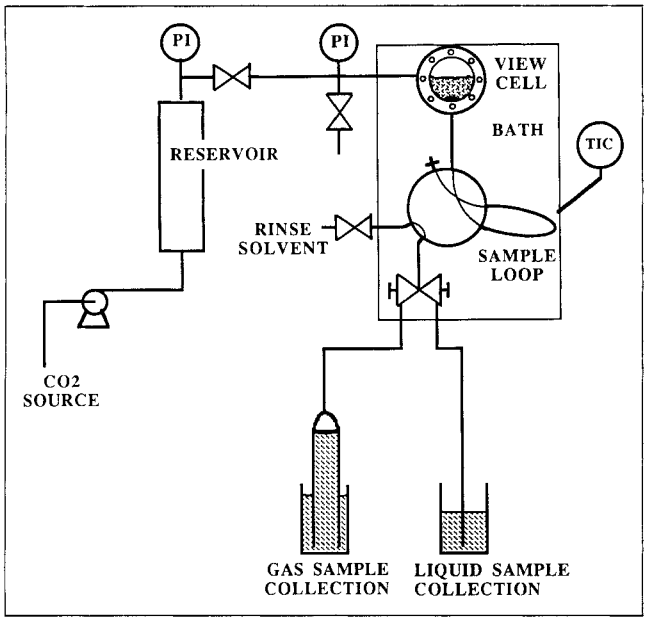

Figure 1. Experimental apparatus for measuring solid-liquid-vapor equilibria.

CO_2 is applicable to a much broader range of solutes than RESS, since it is usually possible to choose an appropriate liquid solvent. Another advantage is the lower pressures for antisolvent crystallization, typically 5–100 bar. Finally, it may be possible to accomplish fractional crystallization by controlling the gas pressure, although this concept has received little attention. In gas antisolvent crystallization, the expansion is much slower and the supersaturation is smaller than in RESS, so that particle sizes are expected to be larger, for example, >100 micron particles have been formed. However, monodisperse crystals of 1 micron or less can be formed by adjusting expansion conditions (Gallagher et al., 1989). An organic solvent is still present, but the gas antisolvent is much easier to recover than a liquid antisolvent and is more environmentally acceptable. Clearly, the two crystallization processes are quite different and complementary. In both processes, an interesting feature is that pressure may be adjusted to control the crystallization over a continuum.

To date, there is relatively little knowledge of the solubilities of solids in liquids expanded with gaseous CO_2. This involves three-phase solid-liquid-vapor (S-L-V) equilibria for ternary and multicomponent systems, which have been reviewed by Luks (1986). Our objective is to develop a predictive molecular thermodynamic model of these solubilities for a solid in a binary solvent mixture. We examine both regular solution theory and an expanded liquid equation of state model. Because the database is scarce, we present a rapid experimental technique to observe phase behavior visually and to obtain microsamples to determine compositions and density. We chose to investigate naphthalene, phenanthrene, and a mixture of the two, which display an ordinary eutectic without forming a solid solution (Stephen and Stephen, 1963). The solubility behavior of these solids in pure toluene and pure CO_2 is well-known (Stephen and Stephen, 1963; Kurnik et al., 1981; Mackay and Paulaitis, 1979). The data indicate that this system is well-suited for further experimental study and for developing and evaluating molecular thermodynamic models. The final objective is to examine the selectivity of fractional crystallization with a gas antisolvent.

This study is also beneficial for understanding the large nonidealities present in supercritical fluid solutions. At low pressures, the solutions are quite close to the ideal liquid solution reference state. The nonidealities grow as the CO_2 concentration in the liquid increases with pressure. Eventually the fluid phase is greater than 90% CO_2, and the organic liquid behaves as a cosolvent in the near-critical fluid.

Experiment

The goal was to design an experiment to include: visual observation of the phase behavior including excess solids, rapid equilibration and sampling, and accurate measurement of the composition and density of the expanded liquid phase. This technique offers several advantages compared with that of Chang and Randolph (1990): visual phase observations were possible, collection of data was relatively fast since disassembly was not required for each data point, excess solids were present in the cell to insure the saturation curve was measured, and a sample loop with a precise known volume was employed to measure the molar volume.

The central feature of the apparatus consisted of a 304 stainless steel vessel with a sapphire window, approximately 28 mL in volume, as shown in Figure 1. Details of the cell are described elsewhere (Lemert et al., 1990; Johnston et al., 1989). The cell was equipped with an egg-shaped Teflon-coated stir bar approximately 3/8 in. (9.5 mm) long by 3/16 in. (4.8 mm) in diameter. The temperature was controlled to within ± 0.1°C with a thermostated water bath. Pressure was generated with a Haskel model AC-152 air-driven gas booster by compressing high-purity carbon dioxide (Liquid Carbonics UHP, 99.99%) and storing it in a 300-mL reservoir. The carbon dioxide was metered through a needle valve (Whitey, SS-21RS4) into the view cell, while the pressure in the vapor phase was measured with an analog pressure gauge (Heise model 54198) to within ± 0.2 bar. Small diameter 316 SS tubing 1/16 in. (1.6 mm) OD $\times$ 0.010 in. (0.25 mm) ID was used to minimize diffusion of the vapor phase into the pressure gauge.

The gas antisolvent experiment began by adding toluene (Fisher, Certified A.C.S.), saturated with a solute such as phenanthrene (Aldrich, 98 + %) or naphthalene (Aldrich, scintillation grade, 99 + %), to the cell. Typically about 2 mL of solution was added. A small amount of solid solute was also added to insure that a solid phase was present. The pressure was raised to the desired value by addition of CO_2, and the system was allowed to equilibrate for at least 30 minutes. A sample of the liquid phase was removed through a 2-μm metallic frit which was installed in the end of a 1/16 in. (1.6 mm) OD, 0.030 in. (0.75 mm) ID, 316 stainless steel tube. The sample was withdrawn with a six-port sampling valve (Valco) and collected in a calibrated sample loop. The sample loop had an internal volume of 73.2 μL $\pm$ 1.3 μL. Because the sample loop volume was small compared to the view cell, pressure drops were less than 0.1 bar. The amount of gas was determined by displacement of CO_2 saturated water in an inverted buret to within 3%. In a separate sample after allowing for re-equilibration, the liquid was flushed from the loop with ethyl acetate and collected in 10-mL ethyl acetate for analysis

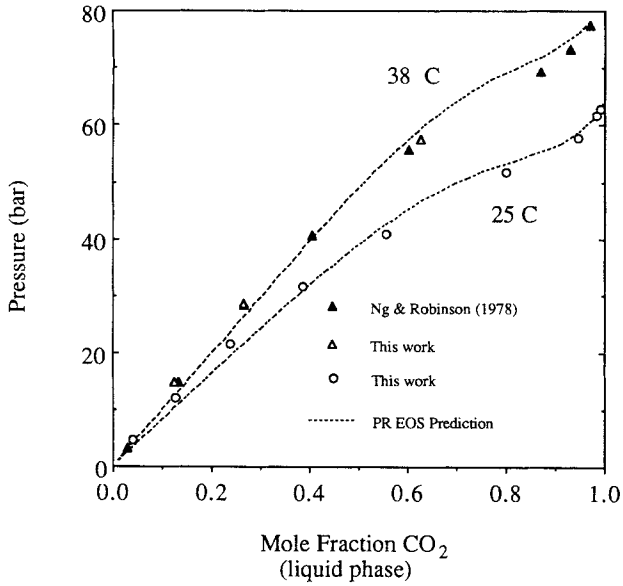

Figure 2. Toluene-carbon dioxide liquid-phase equilibrium compositions: literature data vs. experimental data from this work.

by gas chromatography (GC). Each liquid composition data point was run in triplicate on the GC and then averaged with an average relative percent error of 4%. The GC (Model HP 5890, with model 7673A automatic injector) utilized a capillary column (Lee Scientific, SB-Methyl-100, 25 m) with on-column injection and a FID detector. Hexamethylbenzene (Aldrich, 99+%) was used as an internal reference standard for quantitative analysis of the solute and liquid solvent. It is possible that a few small solid particles could have leaked through the 2-μm metallic frit during sampling. Typical uncertainties in the mole fractions of the components were 3%.

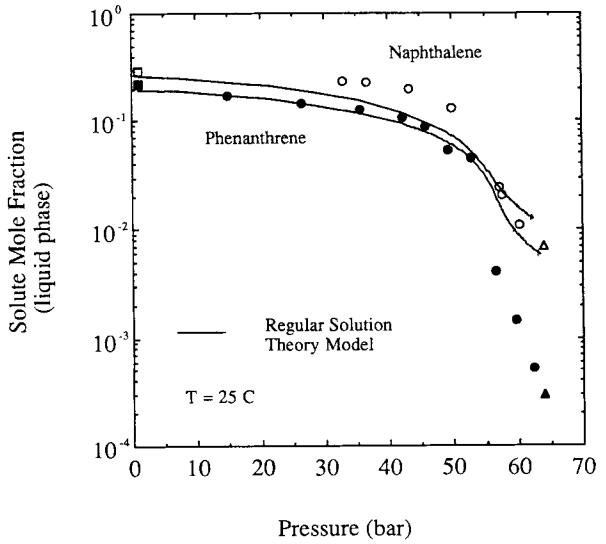

Figure 3. Comparison of experimental and predicted solubilities of naphthalene and phenanthrene in toluene expanded with carbon dioxide.

□, ■, Stephen and Stephen (1963); △, ▲, Johnston (1981); ○, ●, this work.

In the gas antisolvent experiment, after the liquid-phase sample was taken, the pressure was increased to the next value, the system allowed to equilibrate, and the sampling process was repeated. In addition to determination of the liquid mole fractions, the liquid molar volume was also available, since the sample was collected in a known volume. The overall molar volume in the loop was measured with an average relative percent error of 8%. The same approach was used to study systems containing two solids, phenanthrene and naphthalene.

To test the apparatus and experimental procedure, the binary CO_2–toluene system was studied and compared with literature results (Ng and Robinson, 1978). The liquid-phase compositions were measured after equilibrium for 30 minutes.

Results and Discussion

CO_2–toluene phase behavior

Figure 2 shows good agreement between this work and the literature for the CO_2–toluene system at 38°C. The data are correlated accurately with the Peng-Robinson equation of state (PREOS), by using a binary interaction parameter of 0.09 (Ng and Robinson, 1978). New results are also presented at 25°C.

CO_2–toluene-solid phase behavior

The solubilities of naphthalene and phenanthrene in toluene expanded with carbon dioxide are shown in Figure 3 and Table 1. These results show that the mole fraction of the dissolved solid in the liquid phase decreases as the pressure (amount of antisolvent) is increased. Above 45 bar the solubilities begin to fall off sharply. At 60 bar the liquid phase is mostly CO_2 and the mole fractions of the solutes are reduced dramatically. As might be expected based on vapor pressures, naphthalene is more soluble than phenanthrene in the expanded solvent, over the entire pressure region.

At high pressures it would be expected that the solid solubilities should approach those found in pure CO_2. For com-

Table 1. Experimental Compositions and Molar Volumes of the Liquid Phase for Two Ternary Systems at 25°C

Pres. bar	Mole Fraction			Molar Vol. mL/mol
	Toluene	CO_2	Solute	
Toluene-CO_2-Phenanthrene				
14.9	0.682	0.147	0.171	160
26.6	0.579	0.275	0.146	140
35.7	0.496	0.378	0.126	121
42.3	0.424	0.470	0.106	119
45.7	0.371	0.542	0.0870	120
49.2	0.285	0.661	0.0532	124
52.7	0.279	0.676	0.0453	112
56.5	0.0848	0.911	0.00408	84
59.6	0.0343	0.964	0.00146	74
62.4	0.00817	0.991	0.00051	66
Toluene-CO_2-Naphthalene				
32.9	0.429	0.334	0.237	127
36.7	0.398	0.373	0.229	120
43.4	0.346	0.456	0.198	111
49.9	0.277	0.591	0.132	102
57.1	0.0689	0.907	0.0242	74
57.7	0.0510	0.928	0.0209	88
60.3	0.0206	0.969	0.0108	72

parison, Johnston (1981) reported plots of the log of the enhancement factor, $E = y_2P/P_2^{sat}$, vs. density for the CO_2–phenanthrene and CO_2–naphthalene systems. Extrapolation of these data to 25°C at 64 bar gives solubilities of 0.0003 for phenanthrene and 0.007 for naphthalene, compared with our measured values of 0.0005 and 0.011 for the same solids, respectively, in the CO_2–toluene mixture. The somewhat larger values are likely due to the presence of 1–2% toluene in the CO_2, which acts as a cosolvent, and to uncertainties in the extrapolation of the literature data. Extrapolation of the data in Figure 3 to 1 bar, where CO_2 concentrations are negligible, indicates that the mole fractions of naphthalene and phenanthrene approach their reported solubilities in pure toluene at 25°C, 0.294 and 0.221, respectively (Stephen and Stephen, 1963). Thus, the measured data of this work have the correct low- and high-pressure limiting values. Table 1 also presents the experimentally measured molar volumes. The molar volume of the liquid phase decreases as the pressure increases, more specifically as the carbon dioxide mole fraction increases. At pressures greater than 60 bar the liquid phase is mostly CO_2, and for comparison, at 64 bar and 25°C, pure liquid CO_2 has a calculated molar volume of 62 cm^3/mol (Reynolds, 1979).

Because gaseous carbon dioxide dissolves readily into toluene at elevated pressures, it is able to reduce the liquid's solvent strength markedly. Above 45 bar, the sharp drop in solubility can be explained by the expansion of the liquid solvent with CO_2, which has a lower solubility parameter and polarizability per volume (Barton, 1983). The solubility parameter of CO_2 is discussed in detail in the section on regular solution theory. The mixed solvent solubility parameter of the liquid solvent:

$$\bar{\delta}_{12} = \Phi_1\delta_1 + \Phi_2\delta_2 \tag{1}$$

[CO_2(1) + toluene (2)] decreases as CO_2 is added. Figure 4 shows that the solid's solubility can be represented in an approximately linear fashion by the square of the difference between the solute's solubility parameter and the mixed solvent's solubility parameter. The correlation falters at the highest pressures where the CO_2, which is highly expanded and compressible, cannot be described by a constant solubility parameter. Also, the excess volume is no longer small.

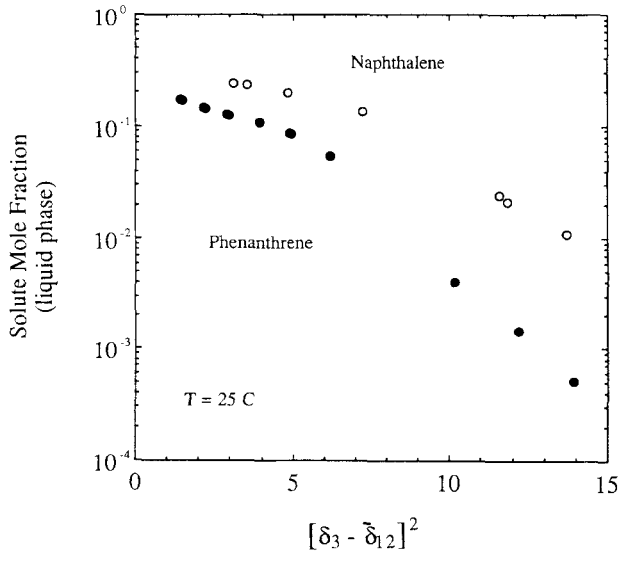

Figure 4. Mole fractions of two solids in toluene expanded with carbon dioxide, correlated with the solubility parameter of the solid and combined solvent.

Thermodynamic modeling of the phase behavior

The CO_2–toluene-solid ternary system at 25°C exhibits three-phase solid-liquid-vapor (S-L-V) equilibria in the pressure range of interest. By establishing the temperature and pressure there are no remaining degrees of freedom, thus the compositions in each of the phases are fixed.

Two simplifying assumptions were made in the model. The solid phase is crystalline and thus assumed to be pure. It was assumed that the solute concentration in the vapor phase was negligible over the range of pressures studied. At higher temperatures and at pressures above the critical pressure of CO_2, the latter assumption becomes less appropriate. However, for the conditions studied, the assumption is reasonable because the vapor pressures for phenanthrene and naphthalene are quite low at 25°C (1.6×10^{-7} bar and 1.1×10^{-4} bar, respectively). Thus, their presence in the vapor phase causes little change in the vapor mole fractions of toluene and CO_2. With these two assumptions there are five unknown mole fractions remaining: carbon dioxide (1) in the vapor and liquid phases, toluene (2) in the vapor and liquid phases, and solute (3) in the liquid phase. Of course, two of these unknowns can be eliminated by the constraint that the mole fractions in each phase must sum to one. Thus, to find the three unknown mole fractions, three independent equilibrium equations are required.

The solvent (2) and gas antisolvent (1) behavior can be described at equilibrium by:

$$y_1\phi_1^V P = x_1\phi_1^L P \tag{2}$$

and

$$y_2\phi_2^V P = x_2\phi_2^L P \tag{3}$$

where ϕ_i is the fugacity coefficient of component (i) in either the liquid (L) or vapor (V) phase, and x_i and y_i are the mole fractions of component (i) in the liquid and vapor phases, respectively. Two models will be considered for the remaining solute equilibrium relationship.

Regular solution theory model

The correlation in Figure 4 suggests regular solution theory (RST) may be used to describe the fugacity of the solute in the liquid phase. It is well-known that RST is appropriate for predicting solubilities of solids in nonpolar liquids (Prausnitz et al., 1986). The solute's behavior at equilibrium can be described by the relationship:

$$f_3^{oS} = x_3\gamma_3 f_3^{oL} \tag{4}$$

where f_3^{oS} and f_3^{oL} represent the fugacities of the pure solid solute and the pure, subcooled liquid solute, respectively, and

Table 2. Physical Properties of Solvent, Antisolvent, and Solids Used to Model Solid-Liquid-Vapor Phase Behavior

Compound	T_m* °C	Δh_f* cal/g	v^{L}** cm³/mol	v^{s} cm³/mol	δ** (cal/cm³)$^{1/2}$	T_c† K	P_c† bar	ω†
CO_2			55		6.014	304.2	73.8	0.225
Toluene			107		8.895	591.7	41.1	0.257
Phenanthrene	100	25.0	158	151.2***	9.774	873††	33.5††	0.536††
Naphthalene	80.3	36.0	131.2	111.9*	9.921	748.35†††	39.7†††	0.302†††

*Perry et al., 1984 **Barton, 1983 ***Dean, 1985
†Prausnitz et al., 1986 ††Reid et al., 1987 †††Henley and Seader, 1981

γ_3 is the solute activity coefficient. It would be perfectly acceptable to describe the solute's behavior with an equation similar to Eq. 2; however, substantial error would arise due to the relatively small size (order of 10^{-6}) of the solute's liquid-phase fugacity coefficient. In other words, the ideal gas standard state is far removed from the actual conditions for a liquid solution.

The regular solution theory model consists of Eqs. 2 through 4. Vapor- and liquid-phase fugacity coefficients were calculated using the Peng-Robinson equation of state (Prausnitz et al., 1986; McHugh and Krukonis, 1986). A binary interaction parameter, k_{12}, was used for the CO_2-toluene pair, and the other k_{ij}'s were set equal to zero. The ratio f_3^{oS}/f_3^{oL} is a function of the solute melting temperature and heat of fusion as described by a standard thermodynamic equation (Prausnitz et al., 1986; Walas, 1985). This equation includes minor heat capacity correction terms which were not included in the calculation. The activity coefficient was determined from RST by assuming that the solubility parameter of hypothetical liquid CO_2 is constant (Barton, 1983; Lemert and Johnston, 1989). Also the solubility parameter and molar volume of the solute were defined with a (hypothetical) subcooled liquid reference state (Table 2). According to regular solution theory (Prausnitz et al., 1986),

$$R\,T \ln \gamma_3 = v_3(\delta_3 - \bar{\delta})^2 \tag{5}$$

where $\bar{\delta}$ is the volume-fraction average solubility parameter, as given by Eqs. 6 and 7, Φ_i is the volume fraction of component i, and v_3 is the hypothetical subcooled liquid molar volume of the solute. The parameters Φ_i and $\bar{\delta}$ are given by:

$$\Phi_i = (x_i v_i^L) / \sum_{j=1}^{3} x_j v_j^L \tag{6}$$

$$\bar{\delta} = \sum_{i=1}^{3} \Phi_i \delta_i \tag{7}$$

The RST model in Table 3 consists of a nonlinear system of equations which were solved simultaneously for each predicted point by use of a numerical equation solver (IMSL, 1987; Garbow, 1980; Brown, 1973). A computer program was written to begin calculations at atmospheric pressure by using an initial solution guess. After the first data point was calculated the pressure was increased by an incremental amount, and the previously calculated compositions provided the initial guess. Convergence would occur providing the pressure step size was not too large. In the highly compressible region, the program would converge if the step size did not exceed 0.05 bar. DiAndreth (1985) found a similar occurrence when modeling multiphase, multicomponent behavior.

Though the model predicts the low- and midpressure solubilities, there is some deviation at the higher pressures, as shown in Figure 3. This can be explained by the inability of RST to describe the solution behavior in the compressible region adequately. However, the high-pressure region appears to be predicted reasonably well for naphthalene, perhaps due to the fact that it is more soluble in pure liquid CO_2 than phenanthrene. RST assumes the components mix with no excess entropy, provided that there is no volume change upon mixing. This assumption breaks down as the CO_2 concentration becomes large and the solution becomes highly compressible. Additionally, the assumption of a geometric mean mixing rule in RST is a severe limitation for the CO_2-naphthalene and CO_2-phenanthrene pairs, which have very different cohesive energy densities. This error is compounded exponentially because of the form of the theory. The geometric mean mixing rule can be relaxed somewhat by including binary interactions coefficients (Prausnitz et al., 1986). These would need to be regressed from binary equilibrium data. However, we found that this gives only modest improvements in the high-pressure region. Another explanation for the deviation comes from the assumption that the solubility parameter of CO_2 is not a function of pressure. Clearly, this is not the case in the highly compressible region where CO_2 is highly expanded (Wong et al., 1985). Even though there are deviations at the higher pressures, this RST model is a simple and useful first approach, giving reasonable results over a modest range of pressure.

Expanded liquid equation of state model

To predict solubilities in the compressible region more accurately an expanded liquid equation of state approach was combined with regular solution theory. To formulate this model, we chose to normalize the solute's fugacity coefficient, ϕ_3, in the low-pressure limit, to avoid large errors associated with values of ϕ_3 on the order of 10^{-6}. This hybrid model utilizes the ability of an equation of state to describe the compressible region while retaining the correct low pressure limit.

At the system temperature and at a reference pressure, P^o, the fugacity of the solute in the liquid phase may be written as:

$$f_3^L(P^o) = x_3\gamma_3(P^o, \{x_i^o\})f_3^{oL} \tag{8}$$

where $\{x_i^o\}$ is the set of mole fractions at the reference pressure. It may also be expressed in terms of a fugacity coefficient with

the relationship:

$$f_3^L(P^o) = x_3\phi_3(P^o,\{x_i^o\})P^o \tag{9}$$

Equating Eqs. 8 and 9 yields:

$$\gamma_3(P^o,\{x_i^o\})f_3^{oL}/\phi_3(P^o,\{x_i^o\})P^o = 1 \tag{10}$$

This factor of unity may be incorporated into Eq. 9 (at pressure P) to yield:

$$f_3^L = x_3\gamma_3(P^o,\{x_i^o\})f_3^{oL}\left[\frac{\phi_3(P,\{x_i\})P}{\phi_3(P^o,\{x_i^o\})P^o}\right] \tag{11}$$

For this work, P^o was chosen as 1 bar so that γ_3, which is described reasonably well by RST, is close to 1 (1.125 for phenanthrene and 1.127 for naphthalene). At P^o the factor in brackets is necessarily unity, reducing Eq. 11 to the conventional expression, Eq. 4. Note that this factor normalizes ϕ_3 at the reference pressure P^o, and consequently this approach predicts the low-pressure region accurately. Then, as the pressure increases the factor in brackets describes the additional nonidealities of the solute in the expanding liquid.

If the molecular thermodynamic models for γ_3, f_3^{oL}, and ϕ_3 were perfect, the ratio in Eq. 10 would always be unity. Because they are not perfect, the incorporation of Eq. 10 provides a normalization of the solute's liquid-phase fugacity coefficient.

The fugacity of the solid at pressure P can be written as:

$$f_3^S = f_3^{oS}\exp\left[\int_{P^o}^{P}\frac{v_3^S}{RT}\,dP\right] \tag{12}$$

At equilibrium, equating Eqs. 11 and 12 leads to the final result:

$$f_3^{oS}\exp\left[\int_{P^o}^{P}\frac{v_3^S}{RT}\,dP\right] = x_3\gamma_3(P^o,\{x_i^o\})f_3^{oL}\left[\frac{\phi_3(P,\{x_i\})P}{\phi_3(P^o,\{x_i^o\})P^o}\right] \tag{13}$$

The fugacity coefficients were calculated with the Peng-Robinson equation of state. Binary interaction parameters were used to describe the CO_2-toluene and CO_2-solute interactions. The CO_2-solute parameters were extrapolated from previous literature data (Kurnik et al., 1981; Mackay and Paulaitis, 1979), and the CO_2-toluene parameter was from Ng and Robinson (1978), as before. Tables 2 and 3 list the pertinent parameters required for the calculations.

Table 3. Calculation Methods and Peng-Robinson Equation of State Binary Interaction Parameters for Regular Solution Theory and Expanded Liquid Equation of State Models

Compound	RST Model	Expanded Liquid EOS Model	Parameters for PR EOS	
			k_{12}	k_{13}
CO_2 (1)	PREOS	PREOS	0.09*	
Toluene (2)	PREOS	PREOS	0.09*	
Phenanthrene (3)	RST	RST + PREOS		0.12**
Naphthalene (3)	RST	RST + PREOS		0.11†

* Ng and Robinson, 1978
**Kurnik et al., 1981
† Mackay and Paulaitis, 1979

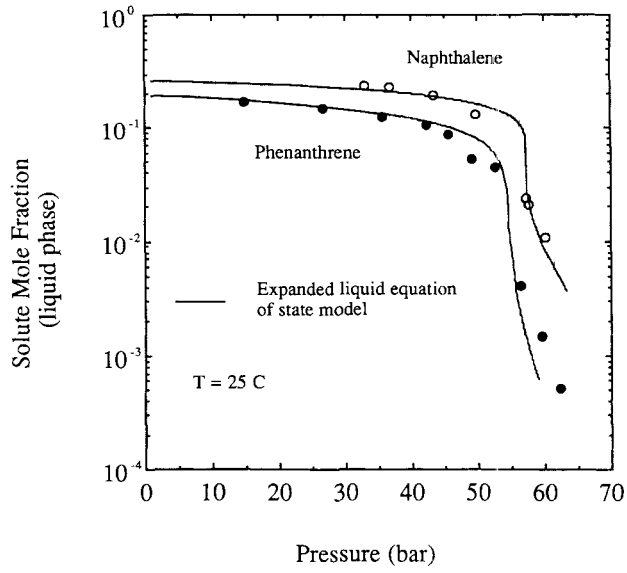

Figure 5. Comparison of experimental and predicted solid solubilities in toluene expanded with carbon dioxide using the expanded liquid equation of state model.

The expanded liquid EOS model is a nonlinear system comprising Eqs. 2, 3, and 13. Table 3 summarizes the calculation methods used in the expanded liquid EOS model, in contrast with the RST model. It is noteworthy that this model uses only binary interaction parameters from the literature; no parameters are fit to the ternary data. Each predicted point is found by simultaneous solution of the system of equations, much like in the RST model. As Figure 5 shows, the solubilities of the solutes are predicted more accurately in the compressible region, while retaining the correct low-pressure limits. Because of the inclusion of an EOS, the predictions are accurate over approximately three orders of magnitude of concentration.

The expanded liquid EOS model presented in this work bridges the gap from near ideal solution behavior to one of a highly nonideal, near critical solution. The model accounts for solute-CO_2 (antisolvent) interactions as well as solvent-CO_2 (antisolvent) interactions. A previous model considered only the latter (Chang and Randolph, 1990). The solute-antisolvent interactions become quite important in the region above about 45 bar for this system, where CO_2 concentrations are large. From 45 to 55 bar the mole fraction of CO_2 in the liquid phase increases from roughly 0.5 to 0.9. The shape of the composition vs. pressure curve is very sensitive to the k_{13} parameter, but less sensitive to k_{12}. Therefore, it is satisfying that the predictions are accurate given the k_{13} values were obtained independently.

Fractional crystallization for the CO_2-toluene-solid (1)-solid (2) system

Because there is a distinct solubility difference between phenanthrene and naphthalene in the CO_2-expanded liquid solvent,

Table 4. Experimental Data Points for the Liquid Phase for the System CO_2-Toluene-Solid 1-Solid 2 at 25°C

Pres. bar	Mole Fraction			
	Toluene	CO_2	Phenanthrene	Naphthalene
12.7	0.343	0.137	0.209	0.311
22.6	0.271	0.240	0.197	0.292
45.5	0.144	0.613	0.105	—
58.7	0.043	0.934	0.004	0.019
61.3	0.015	0.976	0.001	0.007

the potential exists to separate a mixture of the two solutes by manipulation of pressure. Phenanthrene and naphthalene were chosen as model compounds with some foresight toward this objective. These two solids form a eutectic at about 54°C. Thus, at 25°C, when the solids crystallize out of the liquid phase, they will not form a solid solution but rather a physical mixture, assuming that CO_2 does not modify the solid phase. White and Lira (1989) showed that CO_2 at elevated pressures depresses the phenanthrene-naphthalene eutectic; however, no evidence, such as melting of the crystals, was observed in this study. This is consistent with the fact that even at the highest pressures, the temperature was at least 10°C below the eutectics found by White and Lira.

To map out the region available for separation, we began at the limiting point of toluene saturated with both solids at atmospheric pressure. Excess solids were added to insure that the saturation curve was measured. Next, the pressure was increased by adding CO_2 and the liquid composition was measured. This procedure delineated the combined saturation curve of both solids, that is, S-S-L-V equilibria.

Comparison of the experimental results in Table 4 with those with only a single solid present (Table 1) shows that the solid solubilities are higher when the other solid is present. Kurnik and Reid (1982) and Dobbs and Johnston (1987) found a similar trend for pairs of crystalline solids in supercritical CO_2. Sergeeva and Krupnikova (1961) also found that the solubility of naphthalene in methyl alcohol increased upon addition of phenanthrene. For the naphthalene, phenanthrene, toluene, CO_2 system at room temperature we found that the solubility of phenanthrene was about 17% (mole fraction basis) higher and naphthalene about 6% higher than the case where only a single solid was present. This increased solubility trend holds as the liquid is expanded with CO_2. It is likely that the second solid is behaving as a cosolvent for the other, thus explaining the increased solubilities. Dobbs and Johnston (1987) suggested this cosolvent effect and explained it in terms of attractive interaction parameters.

If the liquid CO_2-toluene mixture is considered as a hypothetical pure solvent, then the quaternary data can be shown on triangular coordinates as a "quasi"-ternary system. Figure 6 is an example of such a plot at 25°C and 8.1 bar. This figure only shows the equilibrium between the liquid and solid phases and does not indicate the composition of the vapor phase. The dark circles on the mixed solvent-phenanthrene axis and the mixed solvent-naphthalene axis represent the solubility of each solid in the ternary system (CO_2-toluene-solid), without the other solid present. The dark square inside the triangle is the measured quaternary liquid-phase composition. This point forms one corner of the region representing liquid in equilibrium with two solid phases, with the other two corners being pure phenanthrene and pure naphthalene. There are two other regions shown: one with liquid in equilibrium with pure, solid phenanthrene and the other with liquid in equilibrium with pure, solid naphthalene. As more of the CO_2 antisolvent is added, the liquid-solid-solid region expands toward the mixed solvent corner of the diagram.

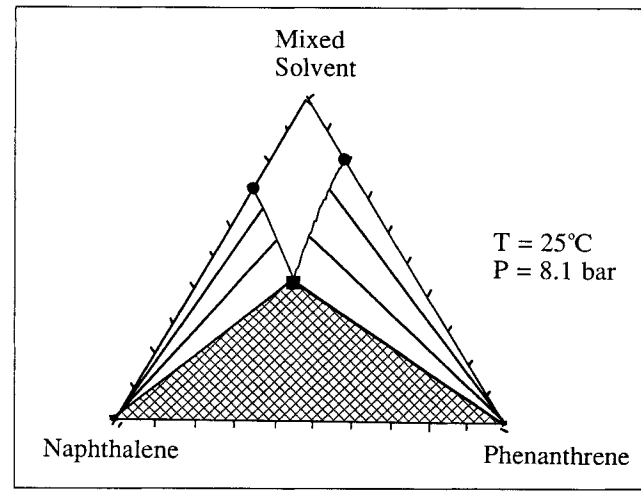

Figure 6. "Quasi"-ternary solid-solid-liquid equilibria for the system CO_2-toluene-naphthalene-phenanthrene.

●, ternary equilibrium this work; ■, quaternary equilibrium this work.

To further visualize the effect of adding antisolvent by increasing the pressure, it is instructive to examine the three-dimensional diagram shown in Figure 7. It is constructed of ternary plots, as in Figure 6, "stacked" from low to high pressure. Here, two surfaces can be seen which represent the equilibrium between liquid and a pure solid. While these sur-

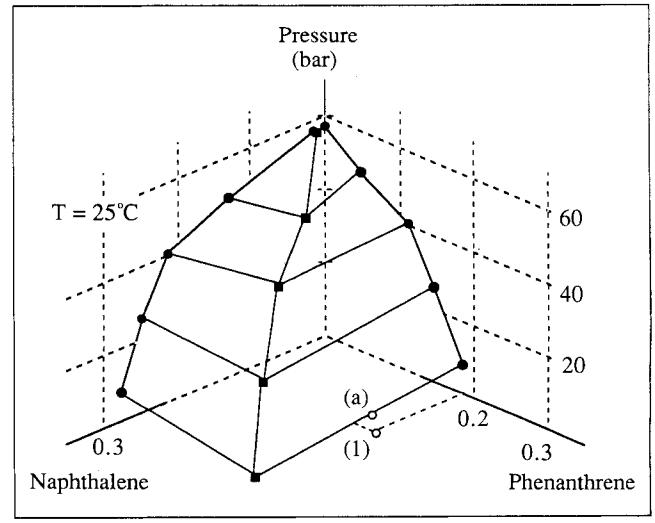

Figure 7. Three-dimensional schematic of a "quasi"-ternary solid-solid-liquid equilibria diagram for the system CO_2-toluene-naphthalene-phenanthrene.

●, ternary equilibrium this work; ■, quaternary equilibrium this work.

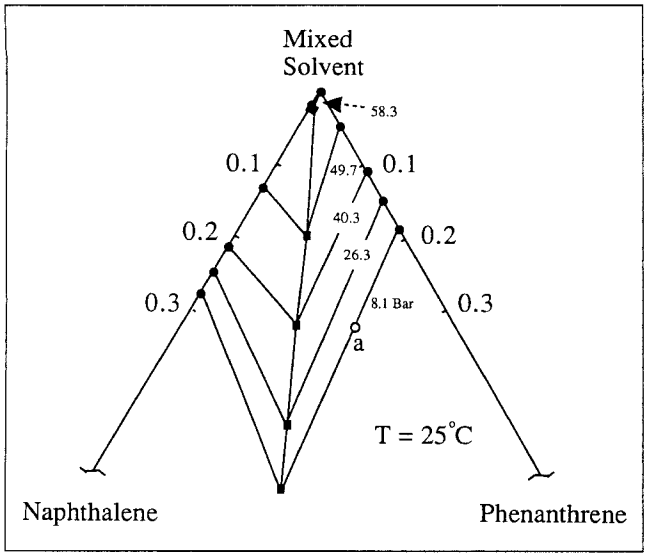

Figure 8. Pressure contours on a "quasi"-ternary solid-solid-liquid equilibria diagram for the system CO_2-toluene-naphthalene-phenanthrene.

●, ternary equilibrium this work; ■, quaternary equilibrium this work.

faces appear to be flat in this illustration, they are likely curved. The endpoints on these surfaces, which intersect the vertical plane drawn through the axis, form the saturation curve (S-L-V equilibrium) of the pure solids in their respective ternary systems, as in Figure 5. The dark circles on these curves are the experimentally measured points. The surfaces represent crystallization surfaces. The intersection of the two surfaces is shown by a line connecting the dark squares. These squares are the experimentally measured quaternary S_1-S_2-L-V equilibrium data points. This line can be described as a pressure eutectic ridge, somewhat analogous to a temperature eutectic trough on a ternary temperature (3-D) diagram (Walas, 1985, p. 415). Along this line both solids crystallize out of solution. For a composition shown by point (1) on Figure 7, there are no solids present since this point is below the crystallization surface. If CO_2 is added, pure phenanthrene crystals form when the composition reaches the crystallization surface. This is somewhat analogous to temperature-controlled crystallization. The difference now is that pressure is the controlling parameter for inducing crystallization. As the pressure is raised by adding CO_2, more solids are precipitated until near 60 bar, when the liquid is mostly CO_2, little solute remains in solution.

Projecting the lines and points from Figure 7 onto a "quasi"-ternary diagram results in Figure 8. On this figure the dark circles and squares again represent experimental points, but now the various isobars are shown as contours. By examining Figures 7 and 8 a path can be described to separate phenanthrene from naphthalene. Suppose one starts with a solution of CO_2, toluene, phenanthrene, and naphthalene, having a composition described by point (1) on Figure 7. At this point only a liquid and vapor phase are present. If the pressure is increased by adding CO_2, the liquid composition will follow along a path until the crystallization surface is intersected at a point (a). At this point pure solid phenanthrene will begin to crystallize out of the solution. As the pressure is further increased, more phenanthrene will crystallize and the liquid-phase composition will move toward the pressure eutectic ridge. When the ridge is reached, solid naphthalene will begin to crystallize out of solution along with the phenanthrene. The amount of phenanthrene crystallized from solution, going from point (a) to the eutectic ridge, can be found from a simple material balance. By stopping short of the eutectic, pure phenanthrene can be recovered by some means such as filtration without any solid naphthalene present. Many other paths can be developed by beginning at different compositions and manipulating the pressure. The diagram also shows that it is possible to recover pure solid naphthalene by operating on the other side of the eutectic.

Since the antisolvent is a gas this raises an interesting potential concept. If a liquid antisolvent had been used and too much had been added, it would be somewhat difficult to remove the extra amount. However, with a gas antisolvent, depressurizing slightly would easily remove the extra antisolvent. Thus, gas antisolvent crystallization can be thought of as reversible simply by releasing some of the gas and subsequently redissolving the solute. This reversibility and adjustability could have utility in redissolving undesirable crystal fines or perhaps for influencing the structure of polymeric membranes. In the previous attempt at using a vapor-phase precipitant in membrane production, the researchers were constrained by slow mass transfer of the antisolvent from the vapor to the liquid phase (Zsigismondy and Bachmann, 1918; Strathmann and Kock, 1977). However, at elevated pressures the vapor phase is much more concentrated and the rate of transfer is likely much faster.

Conclusions

The experimental technique provides a means of determining liquid-phase compositions and density rapidly and accurately, while observing the phases visually. The solubility behavior is treated adequately at low to moderate pressures with regular solution theory, but not at higher pressures where the liquid is nearly pure CO_2, which is highly expanded and compressible. In contrast, the new expanded liquid equation of state model describes the wide range of behavior from the nearly ideal liquid solution at ambient pressure to the highly nonideal compressible fluid. As a result, it predicts solubilities accurately over three orders of magnitude by using only binary interaction parameters. Because the liquid phase becomes mostly CO_2 at higher pressures, the interaction parameter between CO_2 and the solute has a large influence on the predicted solubilities.

The precipitation of solute with added CO_2 may be explained qualitatively in a simple manner with solubility parameters. At 25°C, the solubility parameter of CO_2 in the liquid state is quite low, only 6.0 $(cal/cm^3)^{0.5}$, and it can be substantially lower in the supercritical fluid state. As a result, the addition of CO_2 to nearly any liquid (with which it is significantly miscible) will lower the mixture solubility parameter to a value such that most solutes will precipitate. Only small pressure increases are needed to affect solubilities drastically for pressures above 45 bar.

In systems containing both naphthalene and phenanthrene, each solid acts as a cosolvent for the other, raising solubilities modestly. The solubility of naphthalene in the expanded liquid is much larger than that of phenanthrene, primarily because of its larger vapor pressure. Thus, the selective nature of the gas antisolvent on solubilities may be used for fractional crys-

tallization. Pure solids may be crystallized on either side of a eutectic ridge as a function of pressure, a concept somewhat analogous to thermally-driven crystallization. The potential also exists to create processes capitalizing on the reversibility of the expansion of the solvent with pressure.

Acknowledgment

Acknowledgement is made to the Separations Research Program at the University of Texas, the State of Texas Energy Research in Applications Program, and the Camille and Henry Dreyfus Foundation for a Teacher-Scholar Grant (to KPJ).

Notation

E = enhancement factor
f = fugacity, bar
Δh_f = heat of fusion at the melting temperature, cal/g
k_{ij} = Peng-Robinson equation of state binary interaction parameter
T_m = normal melting temperature of solid, K
v_i = molar volume of component i, cm^3/mol
x,y = mole fraction in liquid and vapor phases, respectively

Greek letters

δ_i = solubility parameter of component i, $(cal/cm^3)^{0.5}$
Φ_i = volume fraction of component i
$\bar{\delta}$ = volume fraction average of the solubility parameter
δ_{12} = mixed solvent solubility parameter
ϕ_i = fugacity coefficient of component i
$\phi_i(P^o,x_i^o)$ = fugacity coefficient evaluated at reference conditions P^o and x_i^o
γ = activity coefficient of solute in the liquid phase
ω = accentric factor

Superscripts

L = liquid phase
o = reference state
s = solid phase
V = vapor phase

Subscripts

1 = carbon dioxide
2 = toluene
3 = solid solute

Literature Cited

Barton, A. F. M., *CRC Handbook of Solubility Parameters and Other Cohesion Parameters*, CRC Press, Boca Raton, FL (1983).
Brown, K. M., "Computer Algorithms for Solving Systems of Simultaneous Nonlinear Algebraic Equations," *Numerical Solutions of Systems of Nonlinear Algebraic Equations*, G. D. Byrne and C. A. Hall, eds., Academic Press, New York (1973).
Chang, C. J., and A. D. Randolph, "Solvent Expansion and Solute Solubility Predictions in Gas-Expanded Liquids," *AIChE J.*, **36**, 939 (1990).
Dean, J. A., ed., *Lange's Handbook of Chemistry*, 13th ed., McGraw-Hill, New York (1985).
DiAndreth, J. R., "Multiphase Behavior in Ternary Fluid Mixtures," PhD Thesis, University of Delaware, Newark (1985).
Dobbs, J. M., and K. P. Johnston, "Selectivities in Pure and Mixed Supercritical Fluid Solvents," *Ind. Eng. Chem. Res.*, **26**, 1476 (1987).
Dobbs, J. M., J. M. Wong, R. J. Lahiere, and K. P. Johnston, "Modification of Supercritical Fluid Phase Behavior Using Polar Cosolvents," *Ind. Eng. Chem. Res.*, **26**, 56 (1987).
Gallagher, P. M., M. P. Coffey, V. J. Krukonis, and N. Klasutis, Garbow, B. S., K. E. Hillstom, and J. J. Moore, *Minpack Project*, Argonne National Laboratory (1980).
Henley, E. J., and J. D. Seader, *Equilibrium-Stage Separation Operations in Chemical Engineering*, Wiley, New York (1981).
IMSL Math/Library, Fortran Subroutines for Mathematical Applications, Houston (1987).
Irani, C. A., C. Cosewith, and S. S. Kasegrande, "New Method for High Temperature Phase Separation of Solutions Containing Copolymer Elastomers," U.S. Patent 4,319,021 (1982).
Johnston, K. P., "Analytical Perturbed Hard Sphere Models Based on Solubility and Volumetric Studies of Organic Solids Interacting with Supercritical Fluids," PhD Thesis, University of Illinois, Urbana-Champaign (1981).
Johnston, K. P., G. J. McFann, and R. M. Lemert, "Pressure Tuning of Reverse Micelles for Adjustable Solvation of Hydrophiles in Supercritical Fluids," *Amer. Chem. Soc., Symp. Ser.*, No. 406 (1989).
Kurnik, R. T., and R. C. Reid, "Solubility of Solid Mixtures in Supercritical Fluids," *Fluid Phase Equil.*, **8**, 93 (1982).
Kurnik, R. T., S. J. Holla, and R. C. Reid, "Solubility of Solids in Supercritical Carbon Dioxide and Ethylene," *J. Chem. Eng. Data*, **26**, 47 (1981).
Lemert, R. M., and K. P. Johnston, "Solid-Liquid-Gas Equilibria in Multicomponent Supercritical Fluid Systems," *Fluid Phase Equil.*, **45**, 265 (1989).
Lemert, R. M., R. A. Fuller, and K. P. Johnston, "Reverse Micelles in Supercritical Fluids. 3. Amino Acid Solubilization in Ethane and Propane," *J. Phys. Chem.*, **94**, 6021 (1990).
Luks, K. D., "The Occurrence and Measurement of Multiphase Equilibria Behavior," *Fluid Phase Equil.*, **29**, 209 (1986).
Mackay, M. E., and M. E. Paulaitis, "Solid Solubilities of Heavy Hydrocarbons in Supercritical Solvents," *Ind. Eng. Chem. Fundam.*, **18**, 149 (1979).
McHugh, M. A., and T. L. Guckes, "Separating Polymer Solutions with Supercritical Fluids," *Macromolec.*, **18**, 674 (1985).
McHugh, M. A., and V. J. Krukonis, *Supercritical Fluid Extraction Principles and Practice*, Butterworths, Stoneham, MA (1986).
Ng, H. J., and D. B. Robinson, "Equilibrium Phase Properties of the Toluene-Carbon Dioxide System," *J. Chem. Eng. Data*, **24**, 325 (1978).
Perry, R. H., D. W. Green, and J. O. Maloney, eds., *Perry's Chemical Engineers' Handbook*, 6th ed., McGraw-Hill, New York, NY (1984).
Prausnitz, J. M., R. N. Lichtenthaler, and E. G. deAzevedo, *Molecular Thermodynamics of Fluid-Phase Equilibria*, Prentice Hall, Englewood Cliffs, NJ (1986).
Reid, R. C., J. M. Prausnitz, and B. E. Poling, *The Properties of Gases and Liquids*, McGraw-Hill, New York (1987).
Reynolds, W. C., *Thermodynamic Properties in SI*, Stanford University, Stanford, CA (1979).
Sergeeva, V., and A. Krupnikova, "Effect of Certain Substances on the Solubility of Naphthalene in Methyl Alcohol," *Shur. Obshchei Khim.*, **31**, 2448 (1961).
Stahl, E., K.-W. Quirin, and D. Gerard, *Dense Gases for Extraction and Refining*, Springer-Verlag, New York (1988).
Stephen, H., and T. Stephen, eds., *Solubilities of Inorganic and Organic Compounds*, Pergamon Press, New York (1963).
Strathmann, H., and K. Kock, "The Formation Mechanism of Phase Inversion Membranes," *Desalination*, **21**, 241 (1977).
Tom, J. W., and P. G. Debenedetti, "Particle Formation with Supercritical Fluids—a Review," *J. Aerosol. Sci.*, **22**, in press (1991).
Walas, S. M., *Phase Equilibria in Chemical Engineering*, Butterworths, Stoneham, MA (1985).
White, G. L., and C. T. Lira, "Four-Phase (Solid-Solid-Liquid-Gas) Equilibrium of Two Ternary Organic Systems with Carbon Dioxide," *Amer. Chem. Soc., Symp. Ser.*, No. 406 (1989).
Wong, J. M., R. S. Pearlman, K. P., Johnston, "Supercritical Fluid Mixtures: Prediction of the Phase Behavior," *J. Phys. Chem.*, **89**, 2671 (1985).
Yu, J. M., S. H. Huang, and M. Radosz, "Phase Behavior of Reservoir Fluids: Supercritical Carbon Dioxide and Cold Lake Bitumen," *Fluid Phase Equil.*, **53**, 429 (1989).
Zsigismondy, R., and W. Bachmann, "Über neue Filter," *Z. Anorg.*